

Roles of anisotropic and unequal gaps in the quasiparticle interference of superconducting iron pnictides

Dheeraj Kumar Singh*

Harish-Chandra Research Institute, Chhatnag Road, Jhansi, Allahabad 211019, India
& Homi Bhabha National Institute, Training School Complex, Anushakti Nagar, Mumbai 400085, India
(Dated: June 30, 2021)

We investigate the role of gap characteristics such as anisotropy and inequality of the gaps in the quasiparticle interferences of iron pnictides using a five-orbital tight-binding model. We examine how the difference in the sensitivities exhibited by the sign-changing and -preserving s -wave superconductivity in an annular region around $(\pi, 0)$, which can be used to determine the sign change of the superconducting gap, gets affected when the gaps are unequal on the electron and hole pocket. In addition, we also discuss how robust these differentiating features are on changing the quasiparticle energy or when the gap is anisotropic.

PACS numbers: 74.70.Xa, 75.10.Lp, 74.55.+v

I. INTRODUCTION

Iron-based superconductors are prototype materials for the multiorbital systems exhibiting magnetism and superconductivity¹. Like cuprates, doping either with electrons or holes leads to the suppression of magnetism and subsequently to the appearance of superconductivity^{2,3}. The symmetry of the superconducting (SC) gap function in this class of materials has been subjected to several theoretical⁴⁻¹³ and experimental investigations, which is suggested to be extended or sign-changing s -wave (s^{+-}). Experimental determination of the sign change is carried out usually by the phase-sensitive measurements using the inelastic-neutron scattering (INS)^{14,15}, the spectroscopic imaging-scanning tunneling microscopy (SI-STM)¹⁶ etc. Latter is a powerful experimental tool and it has been used to investigate the SC gapstructure^{17,32} as well as the normal-state bandstructure¹⁹ in various systems. Recently, it has unraveled the existence of highly anisotropic nanostructures in the SDW state of the electron-doped iron pnictides²⁰⁻²².

Quasiparticle interference (QPI) obtained by the SI-STM depends on the sign change of the SC order parameter across the Fermi surfaces (FSs). This is because the order parameter enters into the coherence factor representing the cooper pair through which the quasiparticle scattering takes place. In the presence of the non-magnetic impurities, the coherence factor is vanishingly small for the scattering vectors connecting those part of the FSs that have same sign of the order parameter. Therefore, the QPI pattern is peaked for only those momenta that connect the part of the Fermi surfaces with the opposite sign of the order parameter²³⁻²⁵. However, the situation is reversed when the impurities are magnetic. In the iron-based superconductor (IBS), QPI in the presence of the magnetic field shows a suppression of the intensity for the scattering vector connecting the electron and hole FSs separated by the magnetic ordering wavevector $\mathbf{Q} = (\pi, 0)$ ¹⁶.

According to the experiments, the electron FS and the inner hole FS are subject to the opening of a larger gap whereas a smaller gap is present at the outer hole FS²⁶⁻²⁹. Moreover, an anisotropic gap has been reported on the electron and hole FSs^{30,31}. These characteristics are expected to play a very im-

portant role in the QPI patterns.

QPIs in the band model³² as well as in the orbital models³³ have been investigated with a focus on the difference of signature of s^{+-} - and s^{++} -wave superconductivity. Some of the above mentioned features for the QPIs when the impurities are either magnetic or non-magnetic have been illustrated for the quasiparticle energy $\omega \sim \Delta$ (SC gap). Particularly in the orbital model, the difference in the patterns near $(\pm\pi, 0)$ and $(0, \pm\pi)$ for the s^{+-} - and s^{++} -wave states was shown to exist within a small energy window around $\omega \sim |\Delta|$, where the SC gap was chosen to be $\Delta \sim 100\text{meV}$ significantly larger than the realistic gap size $\Delta \lesssim 20\text{meV}$. Furthermore, the role of different gaps on the electron and the hole pockets as well as the gap anisotropy was also not explored. A different group of authors using the same model found no noticeable difference between the QPI patterns due to the s^{+-} - and s^{++} -wave state, therefore making the role of QPI ambiguous in distinguishing the s^{+-} - from s^{++} -wave state³⁴. They examined Z map or the Fourier transform (FT) of $(g(\mathbf{r}, E)/g(\mathbf{r}, -E))$ instead of the FT of the tunneling conductance g map ($g(\mathbf{r}, E)$) a quantity directly proportional to the local density of state.

In this paper, we focus on the difference in the g map due to the magnetic and non-magnetic impurities instead of Z map. We show that the difference can be used to determine the sign change of SC order parameter in an unambiguous manner. We find that (i) the s^{+-} - and s^{++} -wave states exhibit robust pattern of differences within a large part of the energy region $\omega \leq \Delta$, where Δ is of the order of observed gap in the experiments. The differences drop rapidly with the quasiparticle energy. (ii) The differentiating features get enhanced at lower energy when either of the gaps on the electron and hole pocket is reduced. (iii) On the other hand, these features are relatively weaker in the case of anisotropic gap. The plan of the paper is as follows. In section II, we describe the procedure to obtain g map. We present results on g maps in the section III due to the non-magnetic and magnetic impurities for both type of s -wave superconductivity. Finally, we present our conclusions in the section IV.

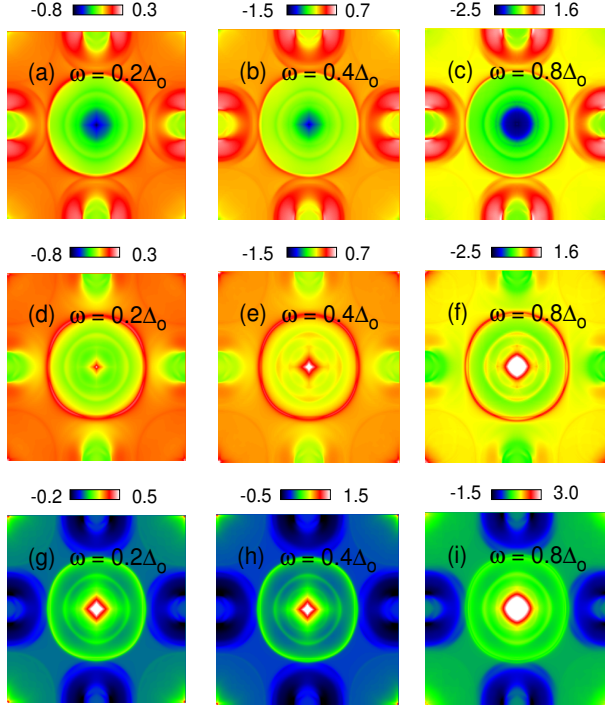


FIG. 1. QPI patterns for the s^{+-} -wave state when the impurity is (a)-(c) non magnetic and (d)-(f) magnetic. (g)-(i) The difference in the QPI patterns due to the magnetic and non-magnetic impurities.

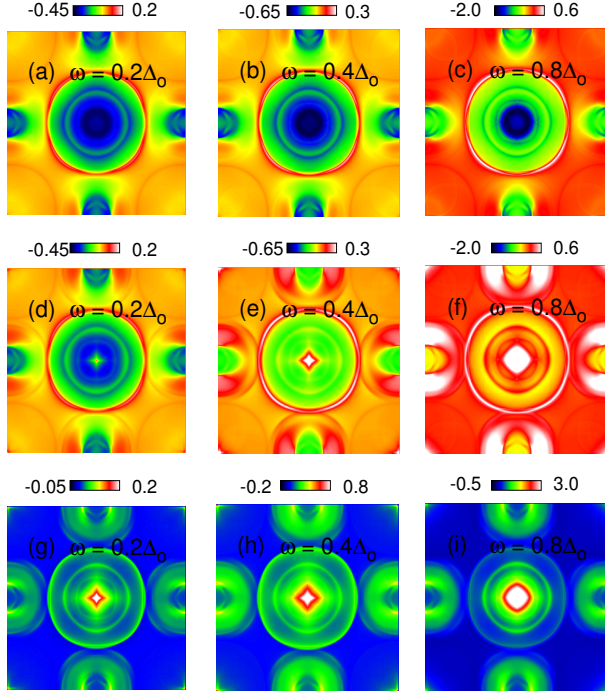


FIG. 2. Same as in Fig. 1 but for the s^{++} -wave state.

II. THEORY

In order to investigate QPIs in the superconducting state, we consider following mean-field Hamiltonian within a five-orbital Hamiltonian

$$\mathcal{H} = \sum_{\mathbf{k}} \Psi^\dagger(\mathbf{k}) \hat{H}(\mathbf{k}) \Psi(\mathbf{k}) = \sum_{\mathbf{k}} \Psi^\dagger(\mathbf{k}) \begin{pmatrix} \hat{\varepsilon}(\mathbf{k}) & \hat{\Delta} \\ \hat{\Delta} & -\hat{\varepsilon}(\mathbf{k}) \end{pmatrix} \Psi(\mathbf{k}), \quad (1)$$

where the electron field operator is defined within the Nambu formalism as $\Psi_{\mathbf{k}\uparrow}^\dagger = (d_{\mathbf{k}1\uparrow}^\dagger, d_{\mathbf{k}2\uparrow}^\dagger, \dots, d_{-\mathbf{k}1\downarrow}, d_{-\mathbf{k}2\downarrow}, \dots)$ with subscript indices 1, 2, 3, 4, and 5 standing for the orbitals $d_{3z^2-r^2}$, d_{xz} , d_{yz} , $d_{x^2-y^2}$, and d_{xy} , respectively. $\hat{\varepsilon}(\mathbf{k})$ is a 5×5 hopping matrix³⁵. $\hat{\Delta}(\mathbf{k})$ is a 5×5 diagonal matrix, where interorbital pairings have been neglected for simplicity. Elements of $\hat{\Delta}(\mathbf{k})$ are given as $\Delta_o^{ii}(\mathbf{k}) = \Delta_o^{ii} \cos k_x \cos k_y$ and $|\Delta_o^{ii} \cos k_x \cos k_y|$ for the s^{+-} - and the s^{++} -wave SC states, respectively.

Impurity-induced contribution to the full Green's function is given by

$$\delta \hat{G}(\mathbf{k}, \mathbf{k}', \omega) = \hat{G}^0(\mathbf{k}, \omega) \hat{T}(\omega) \hat{G}^0(\mathbf{k}', \omega) \quad (2)$$

using standard perturbation theory. Here $\hat{G}^0(\mathbf{k}, \omega) = (\hat{\mathbf{I}} - \hat{H}(\mathbf{k}))^{-1}$. $\hat{\mathbf{I}}$ is a 10×10 identity matrix. Furthermore,

$$\hat{T}(\omega) = (\hat{\mathbf{I}} - \hat{V} \hat{G}(\omega))^{-1} \hat{V}, \quad (3)$$

with

$$\hat{G}(\omega) = \frac{1}{N} \sum_{\mathbf{k}} \hat{G}^0(\mathbf{k}, \omega) \quad (4)$$

and

$$\hat{V} = V_o \begin{pmatrix} \hat{\mathbf{I}} & \hat{\mathbf{O}} \\ \hat{\mathbf{O}} & \pm \hat{\mathbf{I}} \end{pmatrix}. \quad (5)$$

$\hat{\mathbf{I}}$ and $\hat{\mathbf{O}}$ are 5×5 identity matrix and null matrices, respectively. $+$ ($-$) sign in front of the identity matrix is for the magnetic (non-magnetic) impurities, respectively. g map or the fluctuation $\delta N(\mathbf{q}, \omega)$ in the LDOS due to a single delta-like impurity scattering is given by

$$\delta N(\mathbf{q}, \omega) = \frac{i}{2\pi} \sum_{\mathbf{k}} g(\mathbf{k}, \mathbf{q}, \omega) \quad (6)$$

with

$$g(\mathbf{k}, \mathbf{q}, \omega) = \sum_{i \leq 5} (\delta \hat{G}^{ii}(\mathbf{k}, \mathbf{k}', \omega) - \delta \hat{G}^{ii*}(\mathbf{k}', \mathbf{k}, \omega)), \quad (7)$$

where $\mathbf{k} - \mathbf{k}' = \mathbf{q}$.

In the following, the strength of impurity potential V_o is set to be 200meV. Although, we consider a single impurity, the bandfilling n_e is fixed at 6.1. A mesh size of 300×300 in the momentum space is used for all the calculations. Δ_o is taken same for each orbital and it is set to be 20meV throughout. To facilitate a better comparison between the role of the gap sizes and anisotropy, the range of QPI intensity is fixed for each of the s^{++} - and s^{+-} -wave states.

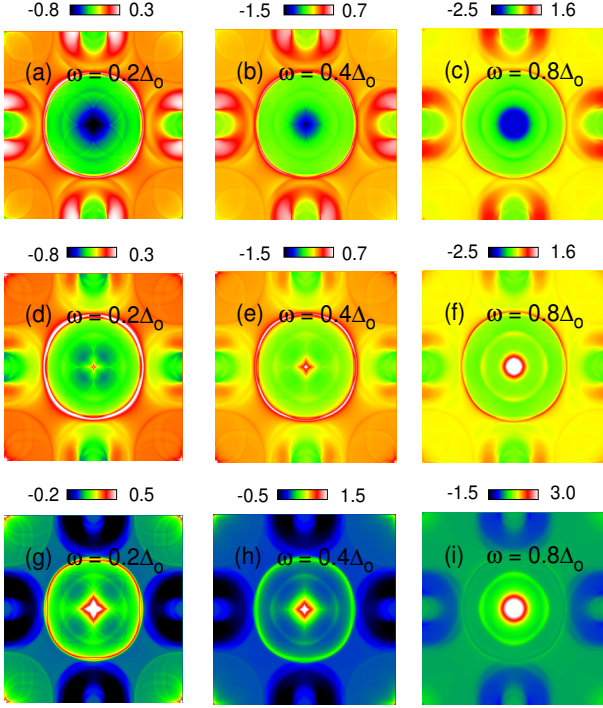


FIG. 3. QPI patterns for unequal gaps $2\Delta_e = \Delta_h = \Delta_o$ in the s^{+-} -wave state when the impurity is (a)-(c) non magnetic and (d)-(e) magnetic. (g)-(i) The difference in the QPI patterns due to the magnetic and non-magnetic impurities.

III. RESULTS

Constant energy contours (CCEs) in the s^{++} - and s^{+-} -wave SC states consist of two concentric pockets around $(0, 0)$ and another pocket around $(\pi, 0)$, which results in several sets of leading scattering vectors. Most of them can be put into three broad categories. First one consists of intrapocket and inter-pocket scattering vectors arising due to the pockets around $(0, 0)$. Second set involves the scattering vectors connecting the pockets around $(0, 0)$ and $(\pi, 0)$. Third one is the set of scattering vectors connecting the CCEs around $(0, -\pi)$ and $(\pi, 0)$. This is a non exhaustive list. For instance, the set of vectors connecting the pocket around (π, π) to other pockets will also contribute to the scattering processes.

First of all, we consider equal gap $\Delta_e = \Delta_h = \Delta_o$, where Δ_e and Δ_h are the SC gaps along the electron and hole pockets, respectively. Fig. 1(a)-(c) and 1(d)-(f) show the QPI patterns in the s^{+-} -wave SC state for the non-magnetic and magnetic impurities, respectively. Results are obtained for several energy values $\omega = 0.2\Delta_o, 0.4\Delta_o$, and $0.8\Delta_o$. Two important differences in the QPI patterns due to the non-magnetic and magnetic impurities can be noticed. First, an annular region around $(\pi, 0)$ and other symmetrically equivalent points are comparatively more intense when the impurity is non-magnetic. Secondly, the sign of the peak at $(0, 0)$ in the case of non-magnetic impurity is opposite to that due to the magnetic

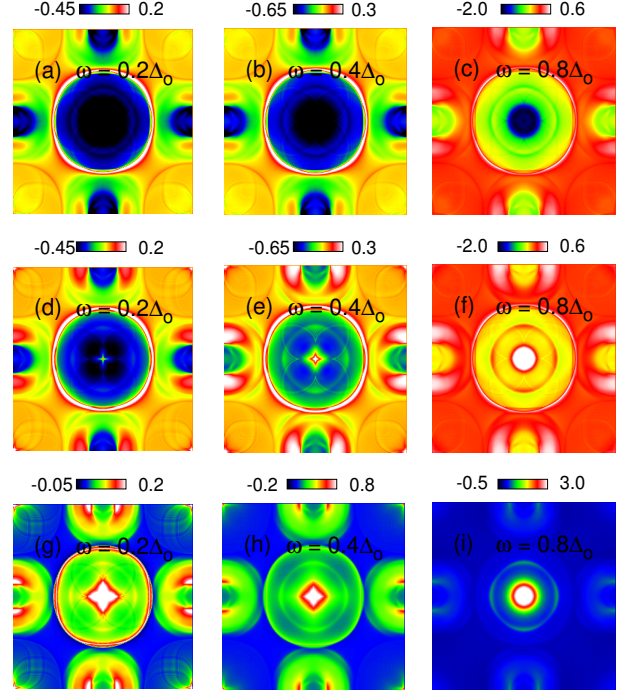


FIG. 4. Same as in Fig. 3 but for the s^{++} -wave state.

impurity. More clarity can be found by plotting the differences of QPI patterns due to the magnetic and nonmagnetic impurities as shown in the Fig. 1(g)-(i), where the peaks are positive and negative around $(0, 0)$ and $(\pi, 0)$, respectively. It is important to note that the differences in the features are more pronounced in the vicinity of $\omega \sim \Delta_o$ and although they are also present at lower energy but weakened relatively.

Fig. 2 shows the QPI patterns when the SC gap has s^{++} -wave symmetry. As can be seen from Fig. 2(a)-(c), the largest negative peak in the non-magnetic case occurs near $(0, 0)$ a feature also present in the patterns for the s^{+-} -wave state. However, the intense and positive annular peak structure around $(\pi, 0)$ occurs now when the impurity is magnetic (Fig. 2(d)-(f)). This is seen more vividly in the differences of the QPI patterns (Fig. 2 (g)-(i)), which is positive in the annular region around $(\pi, 0)$. Therefore, the differences in the QPI patterns due to the magnetic and non-magnetic impurities can be used to determine the sign change of the SC gap.

For simplicity and to focus on individual role, we examine the unequal gaps and anisotropy separately. We consider $2\Delta_e = \Delta_h = \Delta_o$. Similar results are obtained for $2\Delta_h = \Delta_e = \Delta_o$. Fig. 3(a)-(c) show the QPI patterns for the unequal gaps when the impurity is non-magnetic. An important consequence of reducing the gap along the electron pocket is the suppression of intensity in the annular region when $\omega \sim \Delta_o$. However, the intensity grows on decreasing ω in comparison with the equal gap case. As mentioned earlier, when the gaps are equal, QPIs are most intense for $\omega \sim \Delta_o$. Therefore, when one of the gap is reduced, the energy corresponding to the maximum intensity shifts downwards. As a

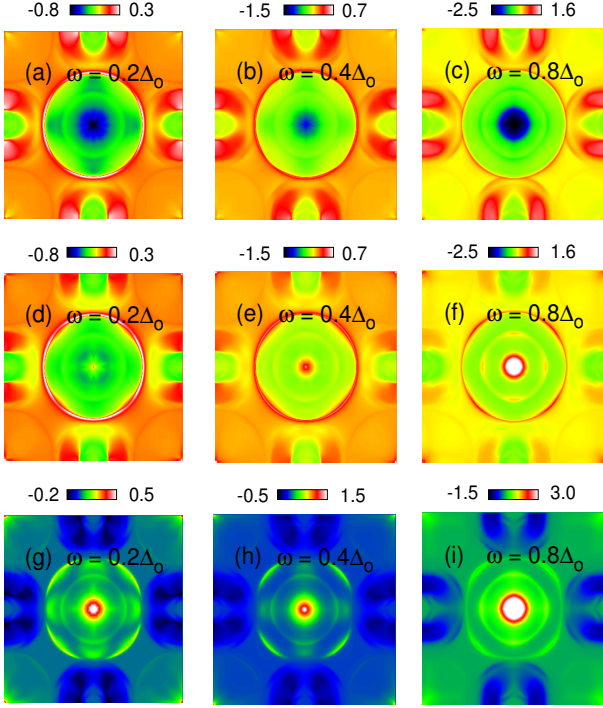


FIG. 5. QPI patterns for the anisotropic gap $\Delta_e = \Delta_o(1 + \cos 2\theta)$ along the electron pocket in the s^{+-} -wave state when the impurity is non magnetic (a)-(c) and magnetic (d)-(e). (g)-(i) The difference in the QPI patterns due to the magnetic and non-magnetic impurities.

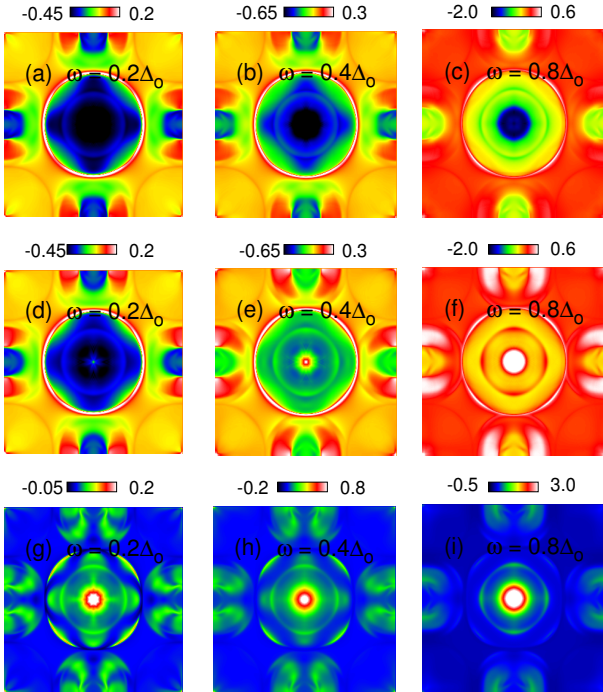


FIG. 6. Same as in Fig. 5 but for the s^{++} -wave state.

result the intensity increases at lower energy. This happens for the annular region around $(\pi, 0)$ even if the impurity is magnetic irrespective of the s^{+-} - or s^{++} -wave states (Fig. 3(d)-(f), Fig. 4(a)-(c), and Fig. 4(d)-(f)). In other words, there is no qualitative difference between the QPI patterns due to the magnetic and non-magnetic impurities. However, increase in the intensity is more in the case of the non-magnetic and magnetic impurities for the s^{+-} - and s^{++} -wave states, respectively. Consequently in comparison with the equal gaps case, differences in the patterns for magnetic and non-magnetic impurities are enhanced especially at lower energy in both type of SC states (Fig. 3(g)-(i), and Fig. 4(g)-(i)).

Fig. 5 and 6 show the QPI patterns for the s^{+-} - and the s^{++} -wave state when the SC gap on the electron pocket is anisotropic. The gap is chosen as $\Delta_e = \Delta_o(1 + \cos 2\theta)$, where θ is defined in such a way that Δ_e is maximum for the point along the line joining $(\pi, 0)$ to $(0, 0)$. The most important effect of the anisotropic gap is that the difference in the QPI patterns due to the magnetic and the non-magnetic impurities diminishes especially at low energy in the annular region around $(\pi, 0)$ (Fig. 5(a)-(f)). In addition, the peak structures are also modified particularly in the annular region. That is well reflected in the plot of differences (Fig. 5(g)-(i)). Similar results are also obtained in the case of s^{++} -wave state (Fig. 6(a)-(i)). Therefore, the difference in the QPI patterns corresponding to the s^{+-} - and s^{++} -wave state also decreases, but the two SC states are still robustly distinguishable.

IV. CONCLUSIONS

In conclusions, we have investigated the QPIs in a five-orbital model of iron pnictides with a focus on the roles of gap features such as inequality and anisotropy. We find that the differentiating features of the s^{+-} - and s^{++} -wave state, which mainly consist of the QPI patterns in an annular region around $(\pi, 0)$, decrease rapidly with the quasiparticle energy, though they are present even at lower energy. The rapid drop is slowed down when one of the gap is reduced, which also results in the widening of the quasiparticle energy range wherein the difference in QPI patterns for two types of superconductivity is enhanced. We also find that appearance of the patterns due to magnetic and non-magnetic impurities are qualitatively similar. Moreover, it is only the difference in the patterns, which is helpful in ascertaining the sign-change of the gap. On the contrary, anisotropic gap leads to the reduction in the differentiating signatures of sign change especially at low energy. Although these characteristics are not responsible for introducing any major qualitative change in the QPI patterns, but they do affect the QPI peak strength in a significant manner.

-
- * dheerajsingh@hri.res.in
- ¹ Kamihara Y., J. Am. Chem. Soc., **130** (2008) 3296.
- ² Dai P., Hu J. and Dagotto E., *Nat. Phys.*, **8** (2012) 709.
- ³ Avcı S. *et. al.*, *Phys. Rev. B*, **85** (2012) 184507.
- ⁴ Cvetkovic V. and Tesanovic Z., *Europhys. Lett.*, **85** (2009) 37002.
- ⁵ Chubukov A. V., Efremov D. V. and Eremin I., *Phys. Rev. B*, **78** (2008) 134512.
- ⁶ Singh D. J. and Du M.-H., *Phys. Rev. Lett.* **100**, (2008) 237003.
- ⁷ Boeri L., Dolgov O. V. and Golubov A. A., *Phys. Rev. Lett.*, **101**, (2008) 026403.
- ⁸ Mazin I. I., Singh D. J., Johannes M. D. and Du M. H., *Phys. Rev. Lett.*, **101**, (2008) 057003.
- ⁹ Wang F., Zhai H. and Lee D.-H., *Phys. Rev. B*, **81** (2010) 184512.
- ¹⁰ Thomale R. *et. al.*, *Phys. Rev. B*, **80** (2009) 180505.
- ¹¹ Kuroki K. *et. al.*, *Phys. Rev. Lett.*, **101** (2008) 87004.
- ¹² Graser S., Maier T. A., Hirschfeld P. J. and Scalapino D. J., *New J. Phys.*, **11** (2009) 025016.
- ¹³ Maier T. A., Graser S., Scalapino D. J., Hirschfeld P. J., *Phys. Rev. B*, **79** (2009) 224510.
- ¹⁴ Lumsden M. D., *Phys. Rev. Lett.* **102** (2009) 107005.
- ¹⁵ Maier T. A., Graser S., Scalapino D. J. and Hirschfeld P., *Phys. Rev. B* **79** (2009) 134520.
- ¹⁶ Hanaguri T., Niitaka S., Kuroki K. and Takagi H., *Science* **328** (2010) 474.
- ¹⁷ Akbari A. and Thalmeier P., *Phys. Rev. B* **88** (2013) 134519.
- ¹⁸ Akbari A., Thalmeier P. and Eremin I., *Phys. Rev. B* **84** (2011) 134505.
- ¹⁹ Lee W.-C., Wu C., Arovas D. P. and Zhang S.-C., *Phys. Rev. B*, **80** (2009) 245439.
- ²⁰ Chuang T.-M. *et. al.*, *Science* **327**, (2010) 181.
- ²¹ Allan M. P. *et. al.*, *Nat. Phys.* **9**, 220 (2013).
- ²² Knolle J., Eremin I., Akbari A. and Moessner R., *Phys. Rev. Lett.* **104**, 257001 (2010).
- ²³ Pereg-Barnea T. *et. al.*, *Phys. Rev. B*, **78** (2008) 020509.
- ²⁴ Maltseva M. and Coleman P., *Phys. Rev. B*, **80** (2009) 144514.
- ²⁵ Sykora S. and Coleman P., *Phys. Rev. B*, **84** (2011) 054501.
- ²⁶ Daghero D. *et. al.* *Phys. Rev. B*, **80**, (2009) 060502(R).
- ²⁷ Tortello M. *et. al.* *Phys. Rev. Lett.*, **105**, (2010) 237002.
- ²⁸ Ding H. *et. al.*, *Europhys. Lett.*, **83**, 47001 (2008).
- ²⁹ Evtushinsky D. V. *et. al.*, *Phys. Rev. B* **79**, (2009) 054517.
- ³⁰ Yoshida T. *et. al.*, *Sci. Rep.*, **4** (2014) 7292.
- ³¹ Umezawa K. *et. al.*, *Phys. Rev. Lett.*, **108**, (2012) 037002.
- ³² Akbari A., Knolle J., Eremin I. and Moessner R., *Phys. Rev. B*, **82** (2010) 224506.
- ³³ Zhang Y.-Y. *et. al.*, *Phys. Rev. B* **80**, (2009) 094528.
- ³⁴ Yamakawa Y. and Kontani H., *Phys. Rev. B*, **92** (2015) 045124.
- ³⁵ Ikeda H., Arita R. and Kunes J., *Phys. Rev. B*, **81** (2010) 054502.